Low Cytoplasmic pH Inhibits Endocytosis and Transport from the *Trans*-Golgi Network to the Cell Surface

Pierre Cosson, Ivan de Curtis, Jacques Pouysségur,* Gareth Griffiths, and Jean Davoust

European Molecular Biology Laboratory, D-6900 Heidelberg, Federal Republic of Germany; and
*Centre de Biochimie CNRS, Université de Nice, Parc de Valrose, 06034 Nice, France

Abstract. A fibroblast mutant cell line lacking the Na^+/H^+ antiporter was used to study the influence of low cytoplasmic pH on membrane transport in the endocytic and exocytic pathways. After being loaded with protons, the mutant cells were acidified at pH 6.2 to 6.8 for 20 min while the parent cells regulated their pH within 1 min. Cytoplasmic acidification did not affect the level of intracellular ATP or the number of clathrin-coated pits at the cell surface. However, cytosolic acidification below pH 6.8 blocked the uptake of two fluid phase markers, Lucifer Yellow and horseradish peroxidase, as well as the internalization and the recycling of transferrin. When the cytoplasmic pH was reversed to physiological values, both fluid phase endocytosis and receptor-mediated endocytosis resumed with identical kinetics. Low cytoplasmic pH also inhibited the rate of intracellular transport from the Golgi complex to the plasma membrane. This was shown in cells infected by the temperature-sensitive mutant ts 045 of the vesicular stomatitis virus (VSV) using as a marker of transport the mutated viral membrane glycoprotein (VSV-G protein). The VSV-G protein was accumulated in the *trans*-Golgi network (TGN) by an incubation at 19.5°C and was transported to the cell surface upon shifting the temperature to 31°C. This transport was arrested in acidified cells maintained at low cytosolic pH and resumed during the recovery phase of the cytosolic pH. Electron microscopy performed on epon and cryo-sections of mutant cells acidified below pH 6.8 showed that the VSV-G protein was present in the TGN. These results indicate that acidification of the cytosol to a pH < 6.8 inhibits reversibly membrane transport in both endocytic and exocytic pathways. In all likelihood, the clathrin and nonclathrin coated vesicles that are involved in endo- and exocytosis cannot pinch off from the cell surface or from the TGN below this critical value of internal pH.

ANIMAL cells maintain a very precise cytoplasmic pH usually between pH 7.0 and 7.2 (reviewed in Roos and Boron, 1981). Growth factors, neurotransmitters, or direct cell–cell interactions can modify the regulation of the intracellular pH in receptive cells (reviewed in Rozengurt, 1986), but little is known about the effect of these variations on membrane traffic. In the case of the endocytic pathway, we showed that the concomitant decrease of the extracellular and intracellular pH inhibits the endocytosis of plasma membrane proteins and fluid phase markers in baby hamster kidney (BHK) cells (Davoust et al., 1987). Clathrin-coated pits, which concentrate receptors and ligands to be internalized, were still present at the cell surface of the acidified cells without apparently being able to pinch off from the cell surface. As a possible interpretation of these data we proposed that clathrin present on coated pits and coated vesicles was unable to depolymerize because of the acidic pH. Another group reported that cytoplasmic acidification inhibits specifically the endocytosis of different receptors located in coated pits, but that the internalization of fluid phase or of ricin which binds to terminal galactose residues was unaffected (Sandvig et al., 1987, 1988). This led to the proposal that an alternative pathway of internalization independent of clathrin-coated pits was responsible for the uptake of ricin or of fluid phase in the acidified cells. In the exocytic direction, a recent report indicated that cytoplasmic acidification can trigger the insertion of proton translocating ATPase in the apical plasma membrane of acid-secreting cells in turtle bladder epithelium (van Adelsberg and Al-Awqati, 1986). These are specialized cells and in the present report, we used fibroblasts to determine whether cytoplasmic acidification could be used to affect differentially the endocytic and exocytic pathways.

To look at several pathways of membrane transport, we assayed simultaneously the internalization and the recycling of ligands, the uptake of two fluid phase markers, and the exocytic transport of a membrane protein from the trans-Golgi

Pierre Cosson's and Jean Davoust's present address is Centre d'Immunologie INSERM-CNRS de Marseille-Luminy, Case 906 13 288 Marseille Cedex 9, France. Ivan de Curtis' present address is Department of Physiology and Howard Hughes Medical Institute, University of California, San Francisco, San Francisco, California 94143-0724.

network (TGN)[1] to the cell surface. We used a mutated cell line, PS120, derived from the hamster lung fibroblast CCL39 cells, which lacks the Na^+/H^+ exchange activity (Pouysségur et al., 1984). These cells could be acidified for 20–30 min using a pulse of NH_4Cl in bicarbonate-free medium followed by a washout. Under the same conditions, the parent cells regulate their cytoplasmic pH because of the activity of the Na^+/H^+ antiport. The mutant cells allowed us to manipulate the intracellular pH without the need of external buffers or substitution of ions, and the parent cells were used to control our experimental conditions. The results indicate that cytoplasmic acidification has an inhibitory effect on the internalization of ligands and markers of the fluid phase, as well as on the export of a membrane protein from the TGN to the cell surface.

Materials and Methods

Materials

FCS, Hepes, horseradish peroxidase (HRP), BSA, transferrin, Lucifer Yellow (LY) CH, and pronase were purchased from Sigma Chemical Co. (St. Louis, MO). Dulbecco's modified essential medium with bicarbonate (DME) or without bicarbonate (DMEb) and Glasgow modified essential medium with bicarbonate (GME) was obtained from Gibco Laboratories (Grand Island, NY). ^{14}C ring-labeled benzoic acid was from Amersham International (Amsersham, UK).

To prepare ^{125}I-labeled transferrin, 0.5 mg of iron-loaded transferrin was diluted in 200 μl PBS (Dulbecco's formulation) and incubated 10 min on ice in the presence of 500 μCi $Na^{125}I$ (Amersham Buchler GmbH, Braunshweig, FRG) in a 20 × 150-mm test tube plated with Iodo-Gen (Pierce Chemical Co., Rockford, IL). The reaction was stopped by removing the sample from the tube and the nonincorporated iodine was removed by chromatography on a Sephadex G50 10 × 0.5-cm column (Pharmacia Fine Chemicals, Piscataway, NJ) equilibrated with PBS supplemented with 0.2% BSA (PBS/BSA). The labeled transferrin (900 cpm/ng) was stored at 4°C and used within 1 month. ^{55}Fe-loaded transferrin (93 cpm/ng) was a generous gift from S. Fuller (EMBL, Heidelberg, FRG).

Cell Cultures and Viruses

CCL39 cell line (American Type Culture Collection, Rockville, MD) and CCL39-derived mutant cell line PS120 lacking functional Na^+/H^+ antiport (Pouysségur et al., 1984) were maintained in DME supplemented with 20 mM Hepes, 4.5 g/liter D-glucose, and 10% FCS (DME/FCS) in a 5% CO_2 incubator. Unless otherwise specified experiments were carried out with 3-d-old confluent cells grown on 5-cm-diam plastic Falcon dishes (~10^7 cells/dish). BHK cells were grown in GME containing 5% FCS, 10% tryptose phosphate broth from Gibco Laboratories, and 10 mM Hepes, pH 7.4 (GME/FCS). 90% confluent monolayers of BHK cells were used after ~2 d of culture. A stock of the clone ts O45-6 of VSV (Griffiths et al., 1985) with a titer of 5.1×10^{11} plaque-forming units (pfu) per ml at 32°C and $< 3 \times 10^5$ pfu per ml at 39.5°C was prepared as described (de Curtis et al., 1988).

Acidification Protocol and Determination of Intracellular pH

To provide an acidification, parent and mutant cells were rinsed with 3 ml DMEb, supplemented with 20 mM Hepes, 4.5 g/liter glucose, and 10% FCS, pH 7.4 (DMEb/FCS), and preincubated at 37°C for 30 min in 3 ml of the same medium containing 20 mM NH_4Cl. The cells were then quickly rinsed twice with DMEb/FCS and incubated in the same medium. The pulse with NH_4Cl was omitted for control experiments.

The measurement of intracellular pH was based on the partition of trace amounts of ^{14}C-labeled benzoic acid between the cytoplasm and the extracellular medium. We used a protocol modified from a previous report (L'Allemain et al., 1984). Briefly, the cells grown in 3.5-cm-diam dishes were incubated for 1 min in 2 ml DMEb/FCS containing 1 μCi [^{14}C]benzoic acid. The dishes were immediately transferred to ice temperature and the cells rinsed four times with PBS within 10 s. After the last wash the cells were extracted for 30 min at 0°C in lysis buffer (10 mM Tris, pH 7.4, 0.05% Triton X-100). The cells were then scraped and homogenized by repeated pipetting through a 1-ml Eppendorf tip. The homogenate was assayed for ^{14}C radioactivity and protein using a Biorad assay (Bradford et al., 1976). The intracellular pH was calculated as previously described (L'Allemain et al., 1984).

Fluid Phase Uptake

LY uptake was tested on cells grown on glass coverslips. LY was used after inactivation of its reactive hydrazine group to reduce the nonspecific background on the cell support. For that, LY was first dissolved in methanol/acetone, 2:1, aliquoted, and dried in defined quantities in 10-ml test tubes. LY was presented to acidified or control cells at 37°C at a concentration of 1 mg/ml. The incubation was stopped at the desired time by chilling the cells which were then rinsed five times with PBS/BSA at 0°C, and photographed in a fluorescence Zeiss photomicroscope equipped with a 63× water immersion lens.

For HRP uptake, parent and mutant cells were incubated in the presence of 1 mg/ml HRP for 5–60 min, then chilled on ice, and washed at 0°C for 5 × 5 min with 20 ml of PBS/BSA and 5 × 5 min with 20 ml of PBS. The amount of internalized HRP was determined as described in a previous report (Davoust et al., 1987).

Transferrin Binding, Uptake, and Recycling

For all the studies using transferrin, 0.2% BSA was substituted for 10% FCS in all the media. The cells were depleted of endogenous transferrin by two washes with 10 ml of DME/BSA followed by three incubations in 10 ml of DME/BSA for 40 min at 37°C in the presence of 5% CO_2 as described (Fuller and Simons, 1986).

To monitor ^{55}Fe uptake, the cells were incubated for 5–60 min in 3 ml DMEb/BSA containing 75 nM of ^{55}Fe-loaded transferrin. They were then cooled on ice and submitted to five cycles of acid and alkaline washes at 0°C: 15 min with 10 ml PBS supplemented with 10% FCS pH 5.0, and 15 min with 10 ml PBS supplemented with 10% FCS pH 8.0 as described (Fuller and Simons, 1986). The cells were then rinsed five times with PBS, extracted at 0°C for 30 min in 500 μl of lysis buffer, scraped, and homogenized. Cellular proteins and radioactivity corresponding to internalized ^{55}Fe were assayed in the lysate.

To monitor the internalization of transferrin at different times after the acidification, the cells were incubated for 5 min at 37°C in 2 ml DMEb/BSA containing 50 nM ^{125}I-labeled transferrin. The cells were cooled on ice to stop the internalization, washed at 0°C 3 × 5 min with 10 ml PBS/BSA and 3 × 5 min with 10 ml PBS, and then treated for 1 h at 4°C with 2 ml pronase solution (DMEb supplemented with 2.5 mg/ml pronase and 20 mM Hepes pH 7.4) to remove ^{125}I-transferrin bound to the cell surface as described (Dautry-Varsat et al., 1983; Ciechanover et al., 1983). The detached cells were resuspended by gentle pipetting through a 1-ml Eppendorf tip, pelleted at 4°C in an Eppendorf microfuge for 5 min, and radioactivity of the total pellet, corresponding to internalized transferrin, was counted. Cellular proteins assayed on separate dishes varied by <10% during the time course of the experiment. Nonspecific internalization was determined in the presence of a 400-fold excess unlabeled transferrin.

To assay the transferrin binding sites on the cell surface, ^{125}I-transferrin was allowed to bind to the cell surface receptors for 90 min using a saturating concentration of 50 nM ^{125}I-transferrin in DMEb/BSA. Unbound transferrin was removed by washing the cells 5 × 5 min with 10 ml PBS/BSA, and 5 × 5 min with 10 ml PBS. The cells were then extracted in 500 μl of lysis buffer, scraped, homogenized, and aliquoted. Cellular proteins and radioactivity were determined. Nonspecific binding was determined in the presence of a 400-fold excess unlabeled transferrin.

To monitor the recycling of transferrin from the endosomes to the cell surface the cells were allowed to internalize ^{125}I-transferrin at a concentration of 50 nM during the pulse with 20 mM NH_4Cl. At time zero the cells were rinsed two times with DMEb/BSA and chased in the same medium for 5–30 min to allow the recycling of ^{125}I-transferrin accumulated in the cells. The dishes were then transferred on ice and the cell medium was collected and replaced with 3 ml of ice-cold PBS/BSA. The cells were then successively washed and treated with pronase, as described for ^{125}I-

1. *Abbreviations used in this paper*: DMEb, Dulbecco's modified essential medium without bicarbonate; GME, Glasgow modified essential medium with bicarbonate; HRP, horseradish peroxidase; LY, Lucifer Yellow; MEMb, minimal essential medium without bicarbonate; TGN, *trans*-Golgi network; VSV-G, vesicular stomatitis virus G protein.

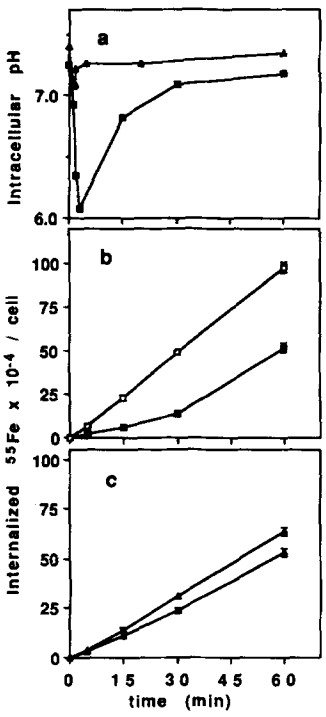

Figure 1. Effect of cytoplasmic acidification on transferrin-mediated ^{55}Fe uptake. Mutant cells lacking the Na^+/H^+ antiport and parent cells were incubated for 30 min at 37°C in the presence of 20 mM NH_4Cl and rinsed twice with a NH_4Cl-free medium. (*a*) Intracellular pH was deduced from the partition of [^{14}C]benzoic acid between the cytoplasm and the extracellular medium at the indicated times after acidification in the mutant cells (■) or the parent cells (▲). (*b*) Uptake of ^{55}Fe in mutant cells incubated in the presence of 75 nM ^{55}Fe-loaded transferrin for the indicated time after acidification (■) or without acidification (□). (*c*) Uptake of ^{55}Fe in parent cells determined as in *b*, after acidification (▲) or without acidification (△). Nonspecific uptake (10%) was determined in the presence of a 400-fold excess of unlabeled transferrin and subtracted from the total counts. The experiments were performed in duplicate and the results expressed as the mean ± SD.

transferrin uptake (Dautry-Varsat et al., 1983; Ciechanover et al., 1983). The total radioactivity of the pellet (pronase resistant counts), of the supernatant (pronase sensitive counts), and of the cell medium was assayed.

Immunofluorescence and Surface Immunoassay of ts O45-infected Cells

Parent and mutant cells were grown on 10 × 10 glass coverslips to ~75% confluency for immunofluorescence or on plastic Petri dishes for the quantitative surface immunoassay. Monolayers were infected with VSV ts O45 at a concentration of 5×10^7 pfu/ml of minimal essential medium without bicarbonate (MEMb) containing 1% FCS and 10 mM Hepes, pH 7.4, for 1 h at 31°C. The virus was discarded and the cells were incubated for 3.5 h at 39°C in DME/FCS. After one wash with DMEb/FCS containing 40 μg/ml of cycloheximide the infected cells were incubated for 105 min in a waterbath at 19.5°C. To acidify the cells, they were rinsed after 75 min at 19.5°C with DMEb/FCS containing cycloheximide and 50 mM NH_4Cl, and incubated in the same medium for another 30 min at 19.5°C. At the end of the 19.5°C incubation, all samples were rinsed twice with DMEb/FCS containing cycloheximide and incubated in the same medium for different times in a waterbath at 31°C. Cells were then cooled on ice and processed for indirect immunofluorescence using a rabbit anti-vesicular stomatitis virus G protein (VSV-G) antibody (K. Simons, EMBL, Heidelberg) followed by incubation with a rhodamine-conjugated goat anti-rabbit IgG antibody (T. Kreis, EMBL). Quantitation of the amount of VSV-G at the cell surface was performed using a new fluoroimmunoassay (Davoust et al., 1987). The monolayer was reacted with a monoclonal antibody against G protein exoplasmic domain (17-2-21-4; K. Simons, EMBL) diluted to 0.5 μg/ml in MEMb for 30 min at 4°C. The cells were then washed 3 × 5 min with PBS containing 0.5% BSA, 1 mM $CaCl_2$, 0.5 mM $MgCl_2$, and treated for 1 h at 4°C with 2.5 ml PBS containing 0.2 μg affinity-purified sheep anti-mouse Fc antibody labeled with Eu (Hemmilä, 1984). The washing sequence was repeated and the monolayer was reacted with 0.5 ml Wallac enhancement solution (Wallac Oy, Turku, Finland) to release the bound Eu and quantitation of the amount of Eu was performed by measuring the delayed fluorescence of 0.2 ml aliquots of the enhancement solution in a Wallac/LKB time-resolved fluorimeter (LKB Instruments, Inc., Gaithersburg, MD).

In another set of experiments, monolayers of BHK cells were infected with VSV ts O45 as described for the PS120 and CCL39 cells. MEMb was substituted for DMEb in the different media and the cells were incubated for 105 min in MEMb/BSA containing 40 μg/ml of cycloheximide in a water bath at 19.5°C. At the end of the 19.5°C incubation, the cells were incubated for 0, 40, or 80 min in a water bath at 31°C either in MEMb/BSA at pH 7.4 or in MEMb/BSA containing 20 mM succinate pH 5.7. To test the reversibility of the treatment at low pH, the monolayers were returned in GME/FCS in the presence of 5% CO_2 at 31°C for 40 min. Quantitation of the amount of VSV-G at the cell surface in nontreated, acid-treated, or reversed cells was performed as for the PS120 and CCL39 cells.

Electron Microscopy and Stereology

Cells were prepared for epon embedding or cryosectioning and immunolabeling as previously described (Griffiths et al., 1983, 1984, 1985).

For the estimation of cell surface coated pits and coated vesicles, 36 random micrographs were taken of epon sections of acidified and control cells at a primary magnification of 28,000. These were enlarged on a projector system that enlarges by a linear factor ×4. The amount of membrane in coated pits (still in obvious continuity with the cell surface) was related to the total amount of plasma membrane by counting the ratio of intersections in both structures (Weibel, 1979). A double lattice grid (D164; Weibel, 1979) was used such that intersections of the total plasma membrane were counted with the large lattice and intersections with coated pits were counted with the small lattice.

Other Assays

The intracellular ATP levels were determined using the luciferin luciferase assay as already described (Davoust et al., 1987).

Results

We first established the conditions of acidification required to inhibit the receptor-mediated uptake of transferrin in mutant cells lacking the Na^+/H^+ antiport and the parent cells were used as a control. To acidify the cytoplasm of both cell lines, we used a pulse of 20 mM NH_4Cl followed by a chase in the absence of NH_4Cl. During the pulse, unprotonated NH_3 diffuses through the plasma membrane and protons generated by cell metabolism or attracted by the intracellular negative potential are captured in the form of NH_4^+. During the chase, the intracellular NH_4^+ dissociates into NH_3, which is permeable, and protons, which cannot cross the plasma membrane. In parent cells, the sodium concentration gradient drives the active extrusion of protons through the Na^+/H^+ antiport at the plasma membrane (L'Allemain et al., 1984), and intracellular pH was only transiently affected after the acidification (Fig. 1 *a, solid triangles*). In mutant cells lacking the functional Na^+/H^+ antiport which were derived from hamster lung fibroblasts (Pouysségur et al., 1984), the acidification of the cytosol reached a pH minimum of 6.2 within the first 2 min of the chase of NH_4Cl and the pH was maintained below pH 6.8 for ~20 min (Fig. 1 *a, solid squares*). This slow recovery of intracellular pH was probably due to a regulation of intracellular pH mediated by trace amounts of HCO_3^- in equilibrium with atmospheric CO_2 as described (L'Allemain et al., 1985). The intracellular ATP level was not affected by cytosolic acidification (data not shown). Cell viability, assayed by counting the cells 24 h after the acidification, was not altered in accordance with previous results (Pouysségur et al., 1984).

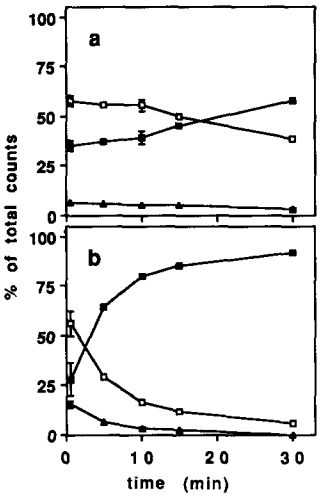

Figure 2. Effect of cytoplasmic acidification on recycling of ^{125}I-labeled transferrin. Mutant and parent cells (*a* and *b*, respectively) were preincubated for 30 min at 37°C with 20 mM NH_4Cl and 50 nM ^{125}I-labeled transferrin. The cells were then washed twice and chased in the absence of NH_4Cl and transferrin. At the indicated times of chase, the amount of ^{125}I-transferrin was determined in the cell medium (free counts; ■), at the cell surface (pronase-sensitive counts; ▲), and inside the cell (pronase-resistant counts; □). Each fraction was expressed as the percentage of total counts that varied from 100,000 to 120,000 cpm per dish. The experiments were performed in duplicate and the results expressed as the mean ± SD.

Cytosolic Acidification Inhibits Receptor-mediated Endocytosis and Recycling to the Cell Surface

We studied the effect of low intracellular pH on the endocytosis and the recycling of transferrin, since this is a well-characterized marker of receptor-mediated endocytosis (Hopkins and Trowbridge, 1983; Dautry-Varsat et al., 1983; Ciechanover et al., 1983; Klausner et al., 1983). The iron-loaded transferrin binds to the transferrin receptor and is internalized via clathrin-coated pits before being delivered to an acidic endocytic compartment. Fig. 1 shows the effect of cytoplasmic acidification on transferrin-mediated ^{55}Fe uptake. In the nonacidified mutant cells, ^{55}Fe accumulates linearly, up to 60 min (Fig. 1 *b, open squares*). The accumulation can be competed by an excess of 1 μM cold transferrin. When mutant cells were acidified at pH 6.2 a significant reduction (80%) in the rate of accumulation of ^{55}Fe was initially detected (Fig. 1 *b, solid squares*). After ~30 min endocytosis resumed at its normal rate. In the wild-type parent cells, ^{55}Fe accumulates at similar rates both with and without acidification (Fig. 1 *c*).

The whole cycle of transferrin internalization and recycling at the cell surface occurs with a half-time of ~7 min (Dautry-Varsat et al., 1983; Ciechanover et al., 1983; Klausner et al., 1983) and it was of interest to determine whether low cytoplasmic pH also had an effect on the recycling from the endosomes to the cell surface. For this purpose, mutant and parent cells were incubated with ^{125}I-transferrin during the 30-min pulse of NH_4Cl and we determined the amount of ^{125}I-transferrin present in the cell medium, inside the cell, or at the cell surface as a function of time during the chase. In the mutant cells acidified at pH 6.2, we observed an inhibition of the recycling to the cell surface of the internalized transferrin (Fig. 2 *a*). Recycling slowly resumed after 20 min, and after 90 min virtually all the internalized counts were released into the cell medium (data not shown). Experiments performed under the same conditions with the parent cells indicated a very rapid and complete exocytosis of ^{125}I-transferrin (Fig. 2 *b*). The same kinetics of transferrin recycling were found in the untreated parent or mutant cells (data not shown). The number of transferrin binding sites at the surface of the mutant cells was not markedly affected by the acidification protocol as quantitated with ^{125}I-transferrin. From 80 to 95% of the control amount of transferrin surface binding sites was detected at different times after the acidification. Furthermore, the proportion of plasma membrane surface area occupied by coated pits was similar in the mutant cells acidified for 10 min or not acidified, respectively, 2.8 ± 0.4% and 2.7 ± 0.5%.

Kinetics of Fluid Phase Endocytosis

To test whether the inhibition of endocytosis was restricted to receptor-mediated endocytosis via coated pits, we used two different fluid phase markers: LY, which can easily be detected by fluorescence microscopy (Swanson et al., 1985), and HRP, which can easily be quantitated (Steinman et al., 1974). In the nonacidified mutant cells, LY accumulated progressively into intracellular vesicles detectable after 10, 20, or 60 min (Fig. 3, *a, b,* and *c*). When the mutant cells were acidified at pH 6.2 no accumulation of the fluid phase marker was detected during the first 10 min (Fig. 3 *d*). Endocytosis resumed after 20 min (Fig. 3 *e*) as evidenced by the presence of fluorescent vesicles in the peripheral cytoplasm. After 60 min numerous intracellular vesicles loaded with LY were detected (Fig. 3 *f*). In the parent cells used as a control, there was no lag time in the formation of LY-positive endocytic vesicles. LY was clearly detectable in endocytic vesicles as bright fluorescent spots, but the quantitation of its uptake was not straightforward because it can slowly permeate the plasma membrane resulting in a weak and diffuse fluorescence in the cytoplasm of the acidified cells (Fig. 3 *d*). To obtain a quantitative estimate of the amount of fluid phase internalized, we used HRP. In the mutant cells without acidification, the accumulation of HRP was continuous for 60 min (Fig. 4 *a, open squares*). In the acidified mutant cells, the uptake of HRP was drastically reduced to 20% of the controls for the first 20 min, and from 30 min onwards endocytosis resumed at its normal rate (Fig. 4 *a, solid squares*). In the parent cells, the uptake of HRP was unaffected by the acidification (Fig. 4 *b*). When mutant cells were acidified and incubated in the presence of bicarbonate and 5% CO_2 to allow the cells to regulate their intracellular pH (L'Allemain et al., 1985), HRP endocytosis resumed within 5 min (data not shown).

We also compared the uptake of HRP with that of ^{125}I-transferrin presented during a 5-min pulse at different times of chase after acidification in the mutant cells (Fig. 5). The uptake of HRP and ^{125}I-transferrin was reduced to one-fifth of the control during the first 20 min of chase. After this time, internalization resumed with superimposable kinetics for both markers indicating that the reduction of intracellular pH below 6.8 had an identical effect on both the fluid phase uptake of HRP and the receptor-mediated endocytosis of transferrin.

Transport of VSV-G from the TGN to the Cell Surface

Since cytosolic acidification clearly interfered with the rate of membrane transport at various stages (internalization and

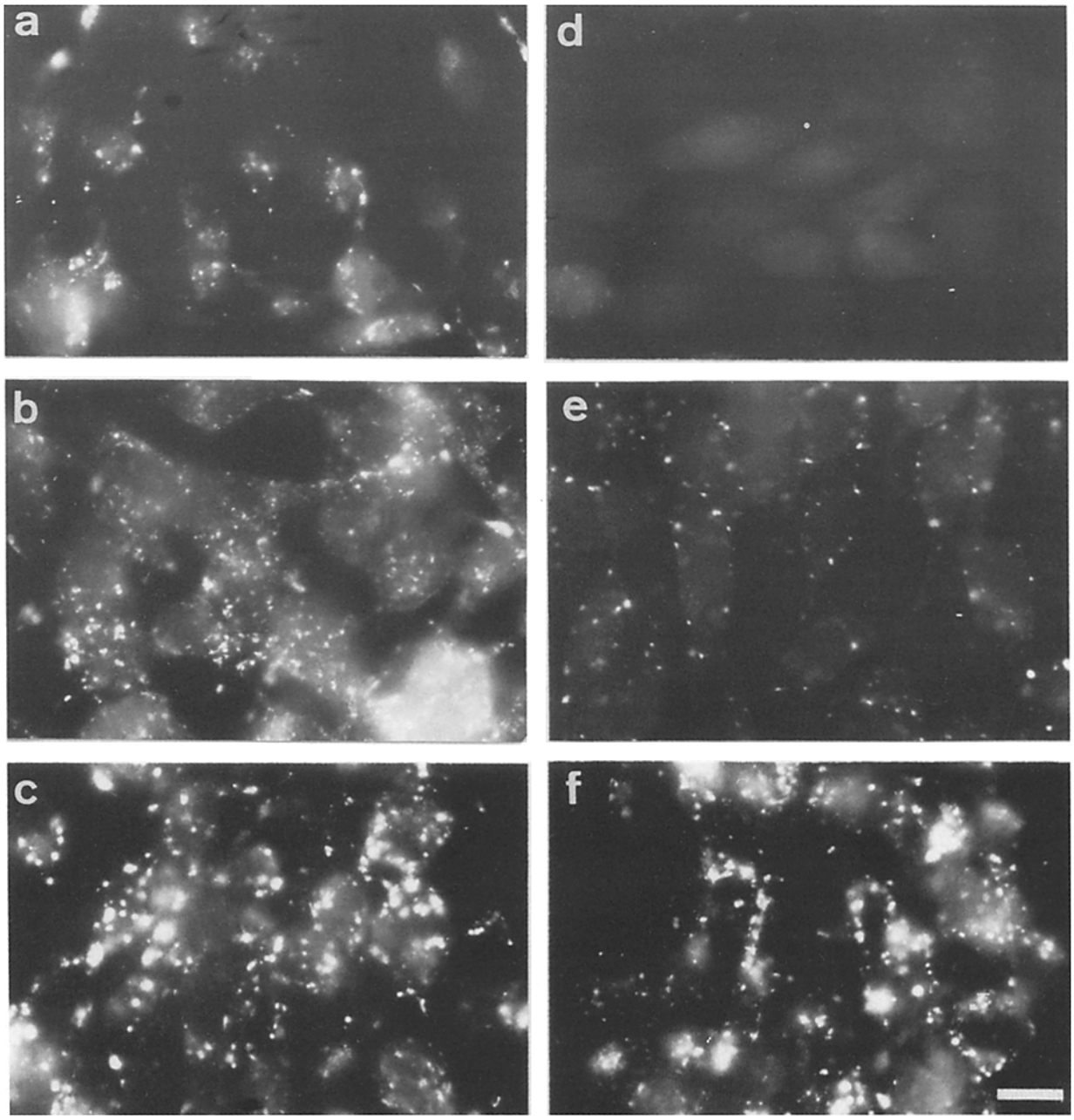

Figure 3. Internalization of LY after acidification of mutant cells. Mutant cells not acidified (*a*, *b*, and *c*) or acidified using a pulse of 20 mM NH_4Cl (*d*, *e*, and *f*) were incubated for different times in the presence of 1 mg/ml of LY. The cells were washed extensively at 4°C before photography using a fluorescence microscope equipped with a fluorescence filter set appropriate for LY and a 63× plan neofluar water immersion lens. Incubation time: 10 (*a* and *d*), 20 (*b* and *e*), and 60 (*c* and *f*) min. Bar, 20 μm.

recycling) in the endocytic pathway, it was conceivable that exocytic transport of proteins might also be affected in a similar way. We took advantage of the temperature-sensitive transport mutant ts O45 of VSV to test the effect of low cytoplasmic pH on the transport of VSV-G from the TGN to the cell surface. The cells were first incubated at the nonpermissive temperature (39°C) to accumulate VSV-G protein in the RER and VSV-G was then accumulated in the TGN for 105 min at 19.5°C in the presence of cycloheximide as previously described (Griffiths et al., 1985; de Curtis et al., 1988). The transport of VSV-G from the TGN to the cell surface was assayed in acidified or nonacidified mutant cells shifted to the permissive temperature of 31°C to allow normal transport of VSV-G protein to the plasma membrane. At 19.5°C, a concentration of 50 mM NH_4Cl (instead of 20 mM at 37°C) was necessary to induce the acidification of the cytoplasm to pH 6.2 when shifting the cells at 31°C. Under these conditions, the variations of intracellular pH with time were equivalent to those established at 37°C (see Fig. 1 *a*).

The transport of VSV-G was monitored either by immunofluorescence in permeabilized cells to reveal its intracellular distribution or by surface immunoassay to quantitate

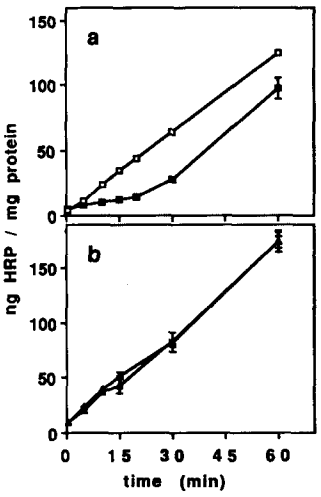

Figure 4. Effect of cytoplasmic acidification on fluid-phase uptake of HRP. Mutant and parent cells were incubated in the presence of 1 mg/ml HRP after acidification with a pulse of 20 mM NH_4Cl or without acidification. At the indicated times the cells were cooled on ice, washed, and the amount of internalized HRP was determined and normalized to the cellular proteins. (*a*) Mutant cells acidified (■) or not (□). (*b*) Parent cells acidified (▲) or not (△). The experiments were performed in duplicate and the results expressed as the mean ± SD.

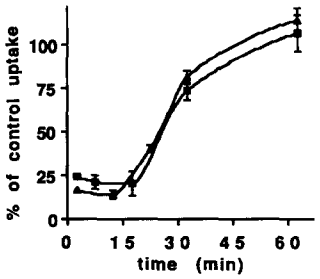

Figure 5. Comparison of fluid phase endocytosis and receptor-mediated endocytosis in acidified mutant cells. Mutant cells acidified with 20 mM NH_4Cl were incubated for different times in DMEb/BSA and then pulsed for 5 min with 1 mg/ml HRP or 50 nM ^{125}I-labeled transferrin. The cells were then cooled on ice, washed, and the internalized HRP (■) or transferrin (▲) were determined. The amounts of HRP or ^{125}I-transferrin uptake are expressed as a percentage of the control (nonacidified mutant cells). In the case of ^{125}I-transferrin, the nonspecific uptake (15% of total determined by an incubation in the presence of a 400-fold excess of unlabeled transferrin) was subtracted and the resulting specific uptake of ^{125}I-transferrin was normalized to the surface binding sites of ^{125}I-transferrin (determined at equivalent time points). The time points indicated on the graph correspond to the midpoint of the 5-min internalization pulses that were used to assay the uptake of HRP and ^{125}I-transferrin.

the rate of appearance of VSV-G at the cell surface. In the Na^+/H^+ mutant cells, VSV-G was localized in the RER at the nonpermissive temperature (Fig. 6 *a*) and then VSV-G moved to the Golgi region after a chase for 105 min at 19.5°C (Fig. 6 *b*). After an additional chase for 30 min at 31°C, most of the VSV-G was present at the surface of the nonacidified mutant cells (Fig. 6 *c*) whereas the VSV-G remained associated with the Golgi region in the acidified mutant cells (Fig. 6 *d*). After 60 min at 31°C, VSV-G was equally present at the cell surface of the nonacidified and acidified mutant cells (Fig. 6, *e* and *f*, respectively). No delay in the transport of VSV-G from TGN to surface was found in the control parent cells treated with a pulse of NH_4Cl (not shown). The time course of the cell surface appearance of VSV-G was determined in either acidified or nonacidified cells using a surface fluoroimmunoassay (Davoust et al., 1987). A half-time of 15 min was found for this process in the nonacidified mutant cells (Fig. 7, *open squares*). Upon cytoplasmic acidifica-

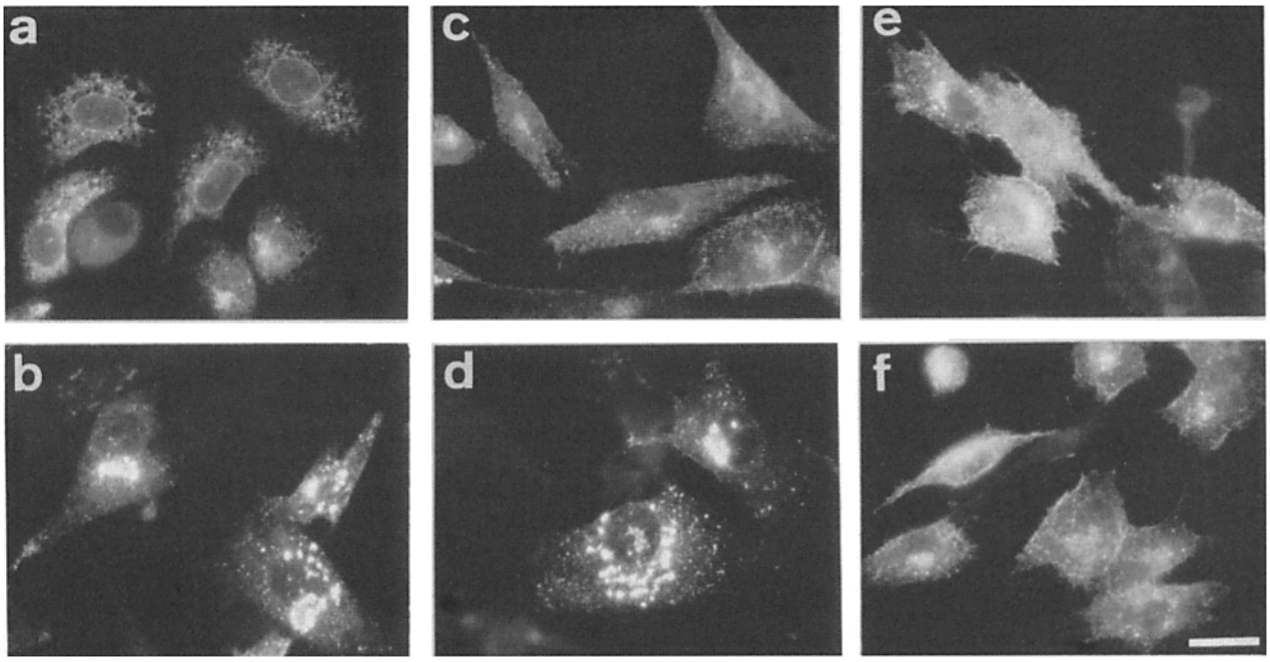

Figure 6. Transport of VSV-G from the TGN to the cell surface in infected mutant cells. Mutant cells were infected with VSV ts O45. VSV-G was accumulated first in the RER for 3.5 h at 39°C (*a*) and then chased to the TGN at 19.5°C in the presence of 40 μg/ml of cycloheximide either for 105 min in nonacidified cells (*b*, *c*, and *e*) or for 75 min followed by 30 min in the presence of 50 mM NH_4Cl for acidified cells (*d* and *f*). Cells were then rinsed twice and either fixed directly (*a* and *b*) or incubated at 31°C in the presence of 40 μg/ml cycloheximide for either 30 (*c* and *d*) or 90 min (*e* and *f*) before fixation. Cells were then processed for immunofluorescence using a rabbit anti-VSV-G antibody followed by a rhodamine-conjugated goat anti-rabbit antibody. Bar, 30 μm.

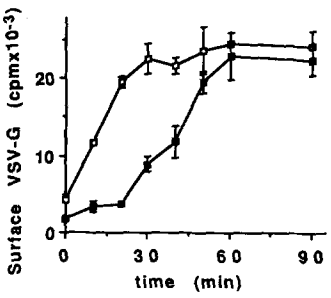

Figure 7. Surface appearance of VSV-G in infected mutant cells. The conditions of infection of mutant cells with VSV ts O45 and the conditions of accumulation of VSV-G in the TGN were identical to the ones of Fig. 6. After the indicated times of chase at 31°C, VSV-G present at the cell surface was quantitated using an anti-VSV-G monoclonal antibody. As a second antibody, we used an Eu-labeled anti-mouse antibody and we measured the delayed fluorescence emission of Eu, using a time-resolved spectrofluorimeter as described previously (Davoust et al., 1987). ■, acidified cells; □, nonacidified cells. Each point was performed in quadruplicate and the results are expressed as a number of photon counts per second ± SD.

tion of mutant cells, the half-time of VSV-G transport to the cell surface was increased to 35 min, but essentially the same amount of VSV-G was delivered to the cell surface after 60 and 90 min as compared to the controls, (Fig. 7, *solid squares*). In the parent cells, the pulse of NH_4Cl had no detectable effects on the rate of appearance of the VSV-G at the cell surface (not shown).

Electron microscopy was then performed either on cryosections labeled with antibodies against the VSV-G to study the intracellular distribution of the VSV-G or on epon sections to observe the morphology of the TGN loaded with VSV-G. On the cryosections obtained from the mutant cells acidified for 30 min (Fig. 8), the gold-labeled VSV-G was present in a membrane compartment indistinguishable from the TGN previously characterized in BHK cells (Griffiths et al., 1985). In agreement with our quantitation of the surface

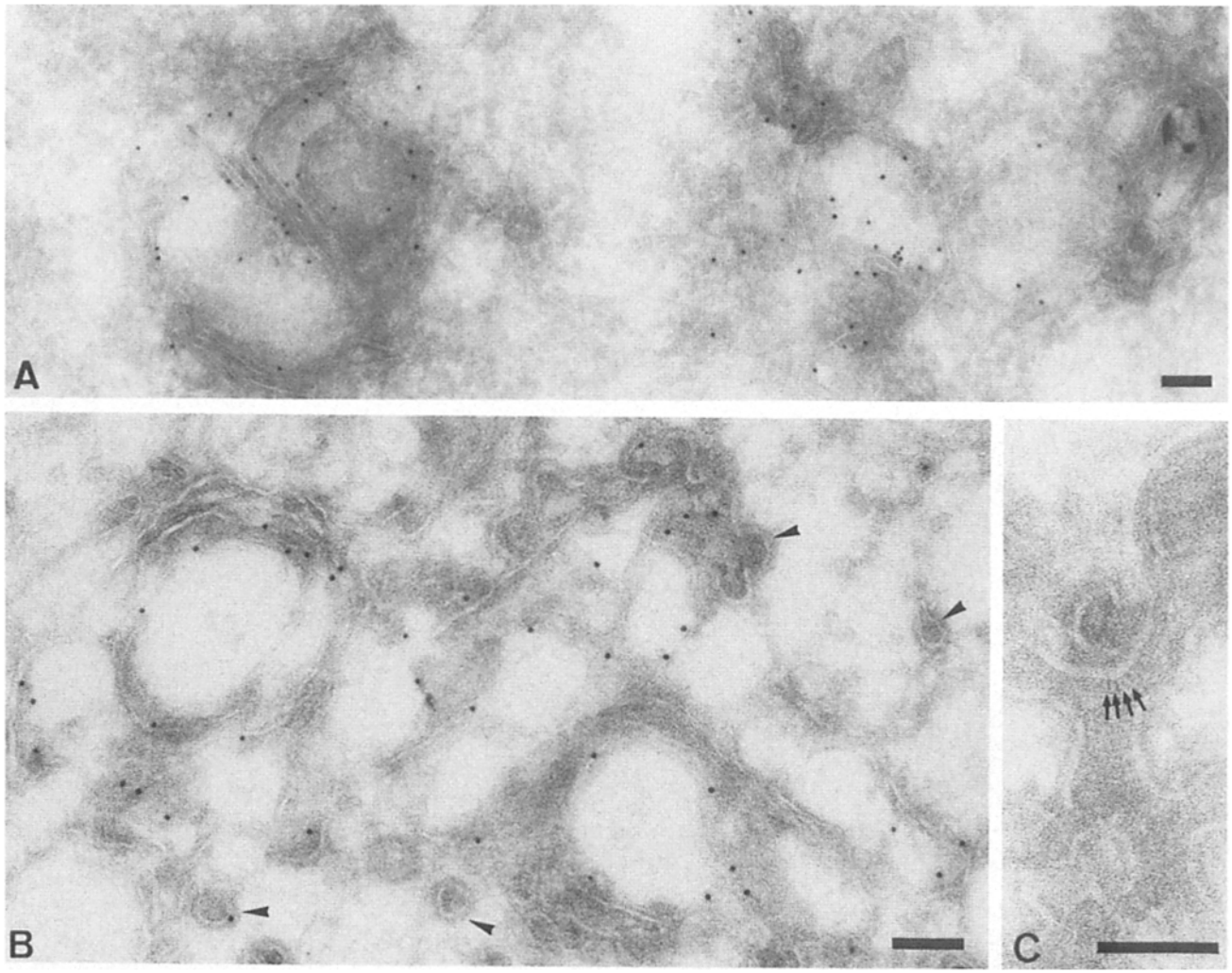

Figure 8. Electron micrographs from cryosections of VSV-infected mutant cells. The conditions of infection, of accumulation of VSV-G at 19.5°C in the TGN and acidification were equivalent to those of Fig. 6. After the pulse of 50 mM NH_4Cl at 19.5°C, the cells were incubated for 30 min without NH_4Cl at 31°C and fixed in 8% formaldehyde. Cells were then processed for cryosectioning and labeled (*A* and *B*) with an affinity-purified antibody against the luminal domain of G protein. Low magnification overview of the Golgi TGN region (*A*) and details of the labeling of the TGN (*B*), evidenced by the presence of numerous coated buds (*arrowheads*). In *C*, a region of the TGN is shown where the structure of the G protein spikes are evident on the luminal side of the membrane. Bars, 100 nm.

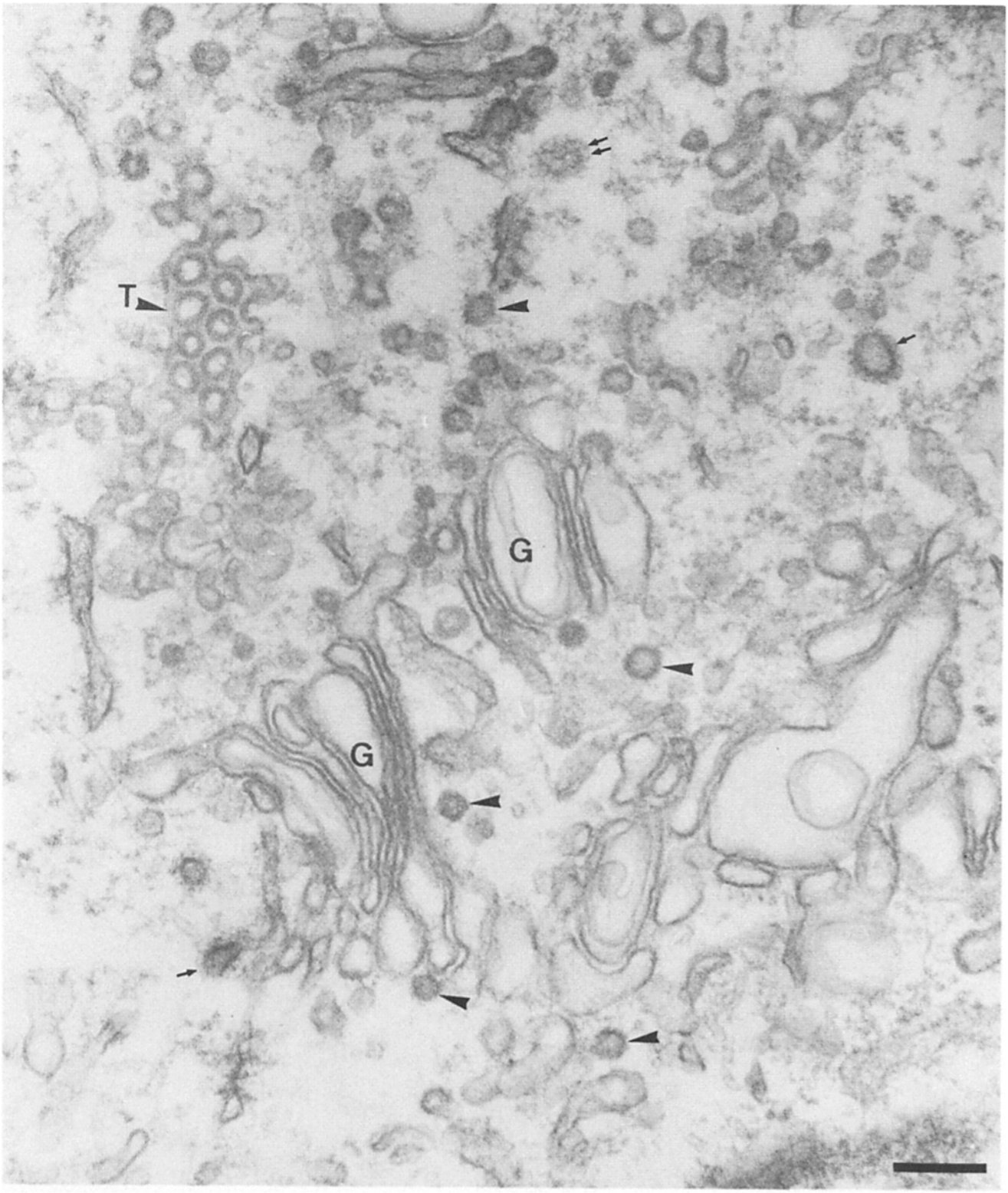

Figure 9. Electron micrograph from an epon section of VSV-infected mutant cells. Epon section of the same preparation as the cryosections in Fig. 8. Note the swollen Golgi stacks (*G*) and extensive TGN region (*T*) which has a distinct thick membrane when filled with VSV-G (see Griffiths et al., 1985). Both clathrin-coated (*arrows*) and nonclathrin-coated (*arrowhead*) vesicular profiles or buds can be seen. The double arrow indicates an oblique section through a clathrin vesicle where the hexagonal lattice is evident. Bar, 200 nm.

VSV-G, there were fewer gold particles at the cell surface as compared to the nonacidified cells (data not shown). On epon sections (Fig. 9), this post-Golgi compartment of accumulation of VSV-G was clearly distinguished from other membranes because of the very dense packing of VSV-G which tends to form invaginations characteristic of the TGN

Table I. Transport of VSV-G from the TGN to the Cell Surface in BHK Cells

Conditions of incubation at 31°C	Intracellular pH	Net amount* of VSV-G transported from the TGN to the cell surface
		counts/s × 10^{-3}
40 min in MEMb pH 5.7	6.2	37 ± 11
80 min in MEMb pH 5.7	6.2	61 ± 21
40 min in MEMb pH 5.7 followed by 40 min in GME‡ pH 7.4	6.2 followed by 7.2	186 ± 15
40 min in MEMb pH 7.4	7.2	148 ± 14
80 min in MEMb pH 7.4	7.2	145 ± 14
40 min in MEMb pH 7.4 followed by 40 min in GME‡ pH 7.4	7.2 followed by 7.2	196 ± 20

BHK cells were infected with VSV ts 045, and VSV-G was accumulated in TGN at 19.5°C under the same conditions as in Fig. 6. Cells were then rinsed twice and incubated at 31°C in the presence of 40 μg/ml cycloheximide as indicated. The amount of VSV-G present at the cell surface was measured with a fluoroimmunoassay as in Fig. 7.

* The background due to the VSV-G transported during the incubation at 19.5°C (32 ± 6 × 10^3 counts/s) was subtracted from the results to monitor only the net amount of VSV-G transported from the TGN to the cell surface during the 31°C incubation. The experiments were performed in triplicate and the results expressed as the mean ± SD.

‡ The BHK cells were incubated with GME/FCS containing bicarbonate in the presence of 5% CO_2 which is needed to reverse membrane transport in cells acidified by exposure to low pH.

loaded with VSV-G (Griffiths et al., 1985). The epon sections indicated also that two types of coated vesicles were still present in the acidified cells in the direct vicinity of the Golgi stacks and the TGN (Fig. 9). The vesicles having a thinner coat are probably equivalent to the nonclathrin-coated vesicles that were shown to contain VSV-G in purified Golgi fractions (Orci et al., 1986; Melançon et al., 1987) and some of them are associated with the rims of the Golgi stacks (see arrowheads in Fig. 9). The vesicles having the thicker coats were most likely clathrin coated (*thin arrows*) and in some cases tangential sections of these revealed the polygonal structure typical of clathrin-coated vesicles (double arrows in Fig. 9). Clathrin-coated and nonclathrin-coated vesicles were also found in the nonacidified cells in approximately equivalent amounts (not shown).

To test whether the inhibition of exocytic transport induced by the low cytosolic pH also occurred in other cell types, we checked the transport of VSV-G in BHK cells acidified by an incubation at an external pH of 5.7 as described (Davoust et al., 1987). Table I shows the quantitation of the VSV-G transported to the surface of BHK cells infected with VSV ts O45 and incubated at 19.5°C under the same conditions used for our parent and mutant cells. When the intracellular pH was dropped to 6.2 at 31°C, the transport of VSV-G from the TGN to the surface was reduced during the first 40 min of acidification to 25% of the control at pH 7.2, and only 41% of the total VSV-G reached the cell surface after 80 min. When the intracellular pH was first dropped to 6.2 for 40 min and then reversed to pH 7.2 in the presence of 5% CO_2, the transport of VSV-G to the surface resumed (126% relative of the control). In the cells incubated for 40 min in MEMb buffered at pH 7.4 and then for 40 min in GME/FCS in the presence of 5% CO_2, we also found a high amount of VSV-G at the cell surface (132% relative to the control).

Discussion

Metabolic inhibitors and reduction in temperature have been used extensively to arrest membrane transport at defined stages in the endocytic and exocytic pathways (reviewed in Mellman et al., 1986; Griffiths and Simons, 1986; Pfeffer and Rothman, 1987). In this study, we examined the effect of cytoplasmic acidification on endocytosis and exocytosis. The Na^+/H^+ antiport deficient cells can easily be acidified and used to study different steps of membrane transport. These cells differ from the parent cells by a point mutation. They are unable to regulate their intracellular pH in the absence of bicarbonate and their cytoplasmic pH can be dropped to pH 6.2 in <2 min using a pulse of 20 mM NH_4Cl followed by an incubation in NH_4Cl-free medium (Pouysségur et al., 1984). The parent cells are not acidified after the pulse of NH_4Cl, and they were used systematically as control cells. We examined in these two cell lines, the effect of cytosolic acidification on the endocytosis and the recycling of transferrin, on the endocytosis of two fluid phase markers, and on the export of a membrane glycoprotein from the TGN to the cell surface.

Influence of Low Intracellular pH on Endocytosis

We showed previously that two threshold values of low extracellular pH could block endocytosis of fluid phase and of plasma membrane proteins at two different stages in BHK cells, an effect that was probably due to the ensuing acidification of the cytosol (Davoust et al., 1987). Under these conditions of low intracellular pH, clathrin formed large intracellular aggregates. We proposed that in the acidified cells, plasma membrane proteins and molecules present in the fluid phase were not delivered to the endocytic compartment because of a strong stabilization of clathrin-coated pits. The same conclusion was reached in Vero or Hep-2 cells which were treated in Na^+ free medium to inhibit the Na^+/H^+ antiport and acidified by a pulse of 40 mM NH_4Cl followed by a chase of 10 min. This treatment lowered the cytoplasmic pH below pH 6.2 and blocked the uptake of HRP-labeled transferrin (Sandvig et al., 1987, 1988). However, when using a pulse of 25 mM NH_4Cl instead of 40 mM, followed by a chase of 30 min instead of 10 min, the endocytosis of LY in the fluid phase or that of ricin-gold conjugates, which binds to galactose-terminating membrane glycoproteins and glycolipids, was not affected by the acidification of the cytoplasm of Vero and Hep2 cells. This finding led to the proposal that nonclathrin-coated pits, also called "smooth" pits, might be responsible for the internalization of LY present in the fluid phase and of ricin bound to terminal galactose residues. Instead, we think that there was a difference in intracellular pH at the different time points considered to analyze the uptake of transferrin, LY, and ricin, and that endocytosis resumed at the longer time points of internalization.

In the Na^+/H^+ antiport deficient cells, we found that endocytosis can be inhibited to about one-fifth of the control by

lowering the cytosolic pH below pH 6.8 and that endocytosis resumes spontaneously after 20 min of acidification when the intracellular pH increases above pH 6.8. The rates of fluid phase endocytosis and of ^{125}I-transferrin endocytosis from the clathrin-coated pits were exactly superimposable at any time point after the initial acidification of the mutant cells (Fig. 4). Therefore, cytoplasmic acidification cannot be used to discriminate different pathways of internalization. Using fluorescent phospholipid analogues implanted at the cell surface in BHK cells, we noticed that the internalization of phospholipids was also reduced to ~20% (Davoust, J. and M. Kail, manuscript in preparation). The internalization of transferrin occurs at a slower rate between pH 6.2 and 6.8 indicating that clathrin-coated vesicles are able to pinch off at a slower rate from the cell surface. The residual internalization of other surface components or of markers present in the fluid phase probably occurs via the same coated vesicles in the acidified cell. In agreement with our interpretation, recent investigations have indicated that the endocytosis of fluid phase and viruses were inhibited to a similar extent in cells loaded with anti-clathrin antibodies (Doxsey et al., 1987). However, we cannot exclude a nonclathrin-coated pathway that would be inhibited at low pH or that would account for <20% of fluid phase uptake. The inhibition of the recycling of ^{125}I-transferrin present in early endosomes indicates that cytoplasmic acidification affects membrane transport at multiple stages in the pathway.

Influence of Low Intracellular pH on Transport from the TGN to the Cell Surface

In the exocytic pathway, several transport vesicles have been clearly identified in close association with the Golgi stacks and the TGN (Griffiths et al., 1985; Griffiths and Simons, 1986). Clathrin-coated vesicles are implicated in the exit of material out of this organel either to the secretory granules (Orci et al., 1984, 1985; Tooze and Tooze, 1986) or to the lysosomes (Lemansky et al., 1987). In addition to clathrin-coated vesicles, a new type of coated vesicle that appears not to contain clathrin has been recently identified in the Golgi complex (Orci et al., 1985; Griffiths et al., 1985). Using Golgi fractions purified from VSV-infected cells and primed with cytosol and ATP, these nonclathrin-coated vesicles were shown to contain VSV-G and it was proposed that these are the carrier vesicles responsible for the constitutive transport of membrane proteins through the Golgi stacks and possibly from the Golgi complex to the cell surface (Orci et al., 1986; Melançon et al., 1987). This finding prompted us to study the transport of VSV-G from the Golgi complex to the cell surface.

To monitor the transport of VSV-G out of the Golgi complex, the cells were infected with VSV ts O45; VSV-G was accumulated in the RER at the nonpermissive temperature of 39°C and then chased to the TGN at 19.5°C as previously described (Griffiths et al., 1985; de Curtis et al., 1988). When the cells were then shifted to the permissive temperature of 31°C, the surface appearance of VSV-G was clearly inhibited by cytosolic acidification for ~30–40 min and resumed afterwards as the cytoplasmic pH increased above pH 7.0. This most likely corresponds to an inhibition of the budding of the carrier vesicles from the TGN for ~20 min followed by a lag time of 10–20 min necessary for the transit of the VSV-G to the cell surface. In BHK cells acidified by exposure to low external pH, the transport of VSV-G from the TGN to the cell surface was also arrested at low cytoplasmic pH and resumed in the presence of a bicarbonate containing medium buffered at pH 7.4.

At the ultrastructural level, VSV-G labeled with immunogold particles on cryosections was clearly associated with a membranous network located in close apposition to Golgi stacks in the mutant cells acidified for 30 min. From its morphology, this intracellular compartment, which retains VSV-G in the acidified cells, is very likely to be the equivalent of the TGN, which has been characterized in details in other cell types (reviewed in Griffiths and Simons, 1986). Furthermore the epon sections revealed the presence of two distinct types of coated vesicles in the Golgi region of the cell. The vesicles having thick and irregular coats are most probably clathrin-coated vesicles whereas, the vesicles having a thinner and more regular coat are often found at the rim of Golgi stacks. This second type of coated vesicles is certainly the equivalent of the nonclathrin-coated vesicles that were recently shown to contain VSV-G in Golgi fractions primed for transport (Orci et al., 1986; Melançon et al., 1987). Since VSV-G was retained in Golgi membranes it is likely that the low cytosolic pH inhibits the formation of carrier vesicles involved in the transport of VSV-G from the TGN to the cell surface.

The VSV-G from the ts O45 mutant can also be used to monitor the transport from RER to Golgi complex by shifting the infected cells from 39 to 31°C. However, we were not able to acidify properly our mutant cells with the NH_4Cl technique during this shift from a bicarbonate-containing medium at 39°C to a bicarbonate-free medium at 31°C. In preliminary experiments, we used BHK cells exposed to an external pH of 5.7 at 31°C and we assayed the appearance of a high molecular weight form of the VSV-G due presumably to sialylation in the TGN (de Curtis et al., 1988). This shift in molecular weight of VSV-G was inhibited at low pH and resumed when returning the cells to neutral pH in a bicarbonate-containing medium as for the transport from the TGN to the cell surface. In all likelihood several processes of membrane budding and transport distributed in the endocytic and exocytic pathways are sensitive to cytoplasmic acidification. However, they might be sensitive to different threshold values of pH beyond the effective resolution of 0.2–0.4 pH unit achieved in our kinetic analysis of membrane transport in the Na^+/H^+ antiport deficient cells. Further experiments are needed to determine the extent of the inhibition of transport from RER to Golgi complex.

In summary the results obtained from the Na^+/H^+ antiport deficient cells indicate that cytosolic acidification below pH 6.8 can inhibit membrane transport in both the endocytic and exocytic directions. The intracellular pH is without doubt an important parameter for cellular functions and membrane traffic is sensitive to defined threshold values of low pH. This can provide new experimental conditions to arrest transiently the export of secretory protein without changing the temperature or the composition of the cell medium. Physiological variations of intracellular pH induced by externally applied growth factors (Pouysségur et al., 1982; Moolenar et al., 1983; Paris and Pouysségur, 1984) or neurotransmitters (Kaila and Voipo, 1987) could also modulate membrane traffic in specialized cells. For example, GABA can cause a drop in postsynaptic pH and it has been proposed that this

might play a role in the inhibition of postsynaptic functions (Kaila and Voipo, 1987). Our results suggest that cytoplasmic acidification could control the efficacy of synaptic transmission by arresting the formation or the release of synaptic vesicles. Future studies will need to focus on the mechanism by which cytoplasmic acidification affect the budding of the clathrin-coated and nonclathrin-coated vesicles involved in endocytic and exocytic processes.

We gratefully acknowledge Mark Kail for excellent technical assistance; Ruth Back for her help in electron microscopy; Ilkka Hemmilä for labeling the affinity-purified sheep anti-mouse Fc antibody with Eu; and Steve Fuller for a generous gift of ^{55}Fe-labeled transferrin. We also thank Jean Gruenberg, Thomas Kreis, and Kai Simons both for their helpful suggestions at various stages of the experiments and for reading drafts of the manuscript. We wish to thank Rachel Wainwright for typing this manuscript with patience and skill.

Received for publication 31 March 1988, and in revised form 7 September 1988.

References

Bradford, M. M. 1976. A rapid and sensitive method for the quantitation of microgram quantities of protein utilizing the principle of protein-dye binding. *Anal. Biochem.* 72:248–254.

Ciechanover, A., A. L. Schwartz, A. Dautry-Varsat, and H. F. Lodish. 1983. Kinetics of internalization and recycling of transferrin and the transferrin receptor in a human hepatoma cell line. Effect of lysosomotropic agents. *J. Biol. Chem.* 258:9681–9689.

de Curtis, I., K. Howell, and K. Simons. 1988. Isolation of a fraction enriched in the trans Golgi network from baby hamster kidney cells. *Exp. Cell Res.* 175:248–265.

Dautry-Varsat, A., A. Ciechanover, and H. F. Lodish. 1983. pH and the recycling of transferrin during receptor-mediated endocytosis. *Proc. Natl. Acad. Sci. USA.* 80:2258–2262.

Davoust, J., J. Gruenberg, and K. Howell. 1987. Two threshold values of low pH block endocytosis at different stages. *EMBO (Eur. Mol. Biol. Organ.) J.* 6:3601–3609.

Doxsey, S., F. M. Brodsky, G. S. Blank, and A. Helenius. 1987. Inhibition of endocytosis by anti-clathrin antibodies. *Cell.* 50:453–463.

Fuller, S. D., and K. Simons. 1986. Transferrin receptor polarity and recycling accuracy in "tight" and "leaky" strains of Madin-Darby canine kidney cells. *J. Cell Biol.* 103:1767–1779.

Griffiths, G., and K. Simons. 1986. The trans Golgi network: sorting at the exit site of the Golgi complex. *Science (Wash. DC).* 234:438–443.

Griffiths, G., K. Simons, G. Warren, and K. T. Tokuyasu. 1983. Immunoelectron microscopy using thin, frozen sections: application to studies of intracellular transport of Semliki forest virus spike glycoproteins. *Methods Enzymol.* 96:466–485.

Griffiths, G., A. McDowell, R. Back, and J. Dubochet. 1984. On the preparation of cryosections for immunocytochemistry. *J. Ultrastruct. Res.* 81:65–78.

Griffiths, G., S. Pfeiffer, K. Simons, and K. Matlin. 1985. Exit of newly synthesized membrane protein from the trans cisterna of the Golgi complex to the plasma membrane. *J. Cell Biol.* 101:949–964.

Hemmilä, I., S. Dakubu, V. M. Mukkala, H. Siitari, and T. Lövgren. 1984. Europium as a label in time-resolved immunofluorometric assays. *Anal. Biochem.* 137:335–343.

Hopkins, C. R., and I. Trowbridge. 1983. Internalization and processing of transferrin and transferrin receptor in human carcinoma A431 cells. *J. Cell Biol.* 97:508–521.

Kaila, K., and J. Voipo. 1987. Post synaptic fall in intracellular pH induced by GABA-activated bicarbonate conductance. *Nature (Lond.).* 330:163–165.

Klausner, C. R., G. Ashwell, J. van Renswoude, J. B. Hardford, and K. R. Bridge. 1983. Binding of apotransferrin to K562 cells: explanation of the transferrin cycle. *Proc. Natl. Acad. Sci. USA.* 80:2263–2266.

L'Allemain, G., S. Paris, and J. Pouysségur. 1984. Growth factor action and intracellular pH regulation in fibroblasts: evidence for a major role of the Na^+/H^+ antiport. *J. Biol. Chem.* 259:5809–5815.

L'Allemain, G., S. Paris, and J. Pouysségur. 1985. Role of a Na^+-dependent $Cl^-/HCO3^-$ exchange in regulation of intracellular pH in fibroblasts. *J. Biol.* Chem. 260:4877–4883.

Lemansky, P., A. Hasilik, K. von Figura, S. Helmy, J. Fishman, R. E. Finne, N. L. Kedersha, and L. Rhome. 1987. Lysosomal enzyme precursors in coated vesicles derived from the exocytic and endocytic pathways. *J. Cell Biol.* 104:1743–1748.

Melançon, P., B. S. Glick, V. Malhotra, P. J. Weidman, T. Serafini, M. L. Gleason, L. Orci, and J. E. Rothman. 1987. Involvement of GTP-binding "G" proteins in transport through the Golgi stack. *Cell.* 51:1053–1062.

Mellman, I., R. Fuchs, and A. Helenius. 1986. Acidification of the endocytic and exocytic pathways. *Annu. Rev. Biochem.* 55:663–700.

Moolenaar, W., R. Tsien, P. Van Der Saag, and S. De Laat. 1983. Na^+/H^+ exchange and cytoplasmic pH in the action of growth factors in human fibroblasts. *Nature (Lond.).* 304:645–648.

Orci, L., P. Halban, M. Amherdt, M. Ravazzola, J.-D. Vassalli, and A. Perrelet. 1984. A clathrin-coated, Golgi-related compartment of the insulin secreting cell accumulates proinsulin in the presence of monensin. *Cell.* 39:39–47.

Orci, L., M. Ravazzola, M. Amherdt, D. Louvard, and A. Perrelet. 1985. Clathrin-immunoreactive sites in the Golgi apparatus are concentrated at the trans pole in polypeptide hormone-secreting cells. *Proc. Natl. Acad. Sci. USA.* 82:5385–5389.

Orci, L., B. S. Glick, and J. E. Rothman. 1986. A new type of coated vesicular carrier that appears not to contain clathrin: its possible role in protein transport within the Golgi stack. *Cell.* 46:171–184.

Paris, S., and J. Pouysségur. 1984. Growth factors activate the Na^+/H^+ antiporter in quiescent fibroblasts by increasing its affinity for intracellular H^+. *J. Biol. Chem.* 259:10989–10994.

Pfeffer, S. R., and J. E. Rothman. 1987. Biosynthetic protein transport and sorting by the endoplasmic reticulum and Golgi. *Annu. Rev. Biochem.* 56:829–852.

Pouysségur, J., J. C. Chambard, A. Franchi, S. Paris, and E. van Obbergen-Schilling. 1982. Growth factor activation of an amiloride sensitive Na^+/H^+ exchange system in quiescent fibroblasts: coupling to ribosomal protein S6 phosphorylation. *Proc. Natl. Acad. Sci. USA.* 81:4833.

Pouysségur, J., C. Sardet, A. Franchi, G. L'Allemain, and S. Paris. 1984. A specific mutation abolishing Na^+/H^+ antiport activity in hamster fibroblasts precludes growth at neutral and acidic pH. *Proc. Natl. Acad. Sci. USA.* 81:4833–4837.

Ross, A., and W. F. Boron. 1981. Intracellular pH. *Physiol. Rev.* 61:296–434.

Rozengurt, E. 1986. Early signals in the mitogenic response. *Science (Wash. DC).* 234:161–166.

Sandvig, K., S. Olsnes, O. W. Petersen, and B. van Deurs. 1987. Acidification of the cytosol inhibits endocytosis from coated pits. *J. Cell Biol.* 105:679–689.

Sandvig, K., S. Olsnes, O. W. Petersen, and B. van Deurs. 1988. Inhibition of endocytosis from coated pits by acidification of the cytosol. *J. Cell Biochem.* 36:73–81.

Steinman, R. M., J. M. Silver, and Z. A. Cohn. 1974. Pinocytosis in fibroblasts. *J. Cell Biol.* 63:949–969.

Swanson, J. A., B. D. Yrinec, and S. C. Silverstein. 1985. Phorbol esters and horseradish peroxidase stimulate pinocytosis and redirect the flow of pinocytosed fluid in macrophages. *J. Cell Biol.* 100:851–859.

Tooze, J., and S. A. Tooze. 1986. Clathrin-coated vesicular transport of secretory proteins during the formation of ACTH-containing secretory granules. *J. Cell Biol.* 103:839–850.

van Adelsberg, J., and Q. Al-Awqati. 1986. Regulation of cell pH by Ca^{+2}-mediated exocytic insertion of H^+-ATPases. *J. Cell. Biol.* 102:1638–1645.

Weibel, E. R. 1979. Stereological methods. I. Practical methods for biological morphometry. Acad. Press Inc., New York. 318 pp.